Relating ^{139}La Quadrupolar Coupling Constants to Polyhedral Distortion in Crystalline Structures

*Alexander L. Paterson, Margaret A. Hanson, Ulrike Werner-Zwanziger, Josef W. Zwanziger**

Department of Chemistry, Dalhousie University, PO Box 15000, Halifax, NS B3H 4R2, Canada

*Corresponding author.

Tel: +1 (902) 494-1960. Fax: +1 (902) 494-1310. E-mail: jzwanzig@dal.ca

Table of Contents

Powder X-Ray Diffraction

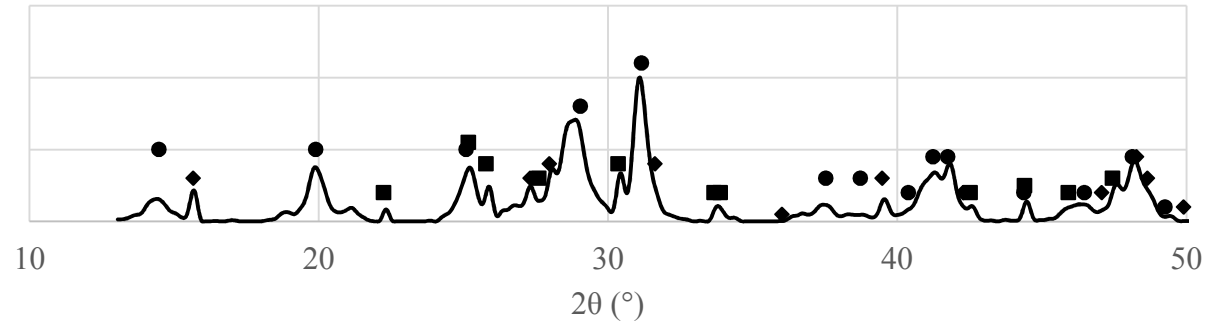

Figure S1. pXRD diffractogram of $LaPO_4 \cdot 1.8H_2O$. Circles (●) indicate peaks from $LaPO_4 \cdot 0.5H_2O$ (PDF 46-1439). Squares (■) indicate peaks from $La_2O_2CO_3$ (PDF 84-1963). Diamonds (♦) indicate peaks from $La(OH)_3$ (PDF 36-1481).

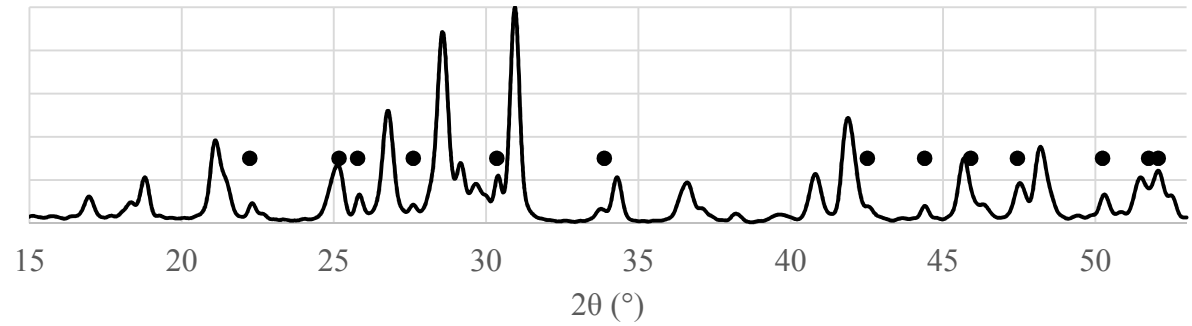

Figure S2. pXRD diffractogram of $LaPO_4$. Circles (●) indicate peaks from $La_2O_2CO_3$ (PDF 84-1963). All other peaks are from $LaPO_4$ (PDF 83-651).

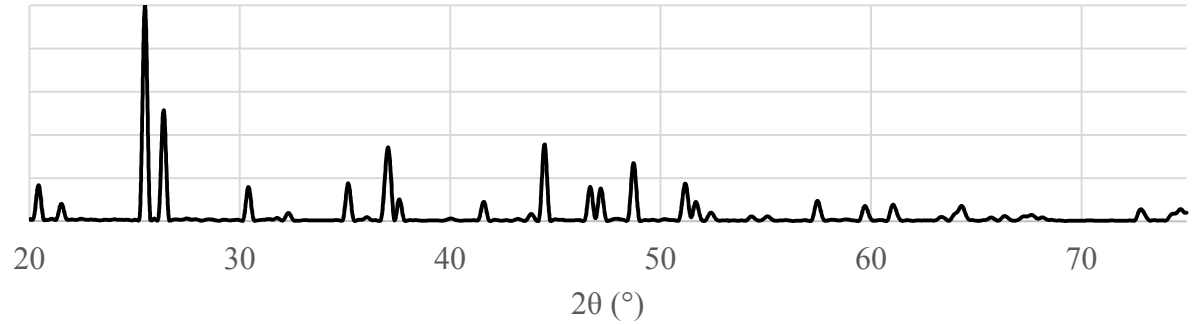

Figure S3. pXRD diffractogram of $LaBO_3$. All observed peaks are from $LaBO_3$ (PDF 12-0762).

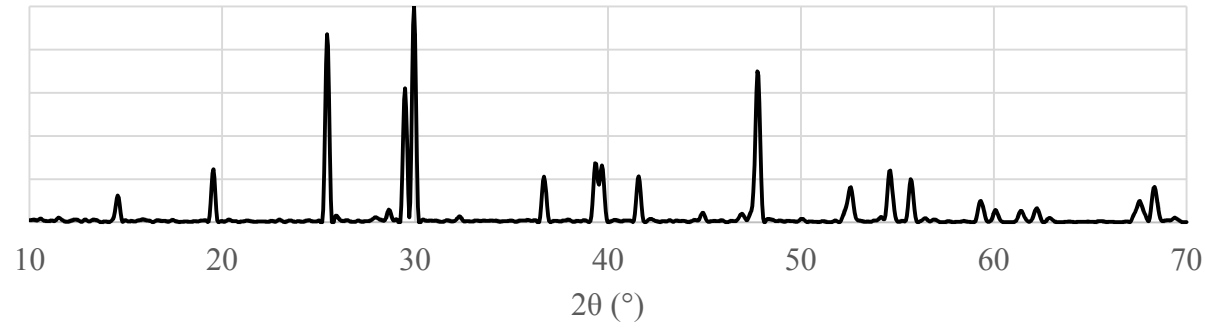

Figure S4. pXRD diffractogram of $LaBGeO_5$. All observed peaks are from $LaBGeO_5$ (PDF 41-659).

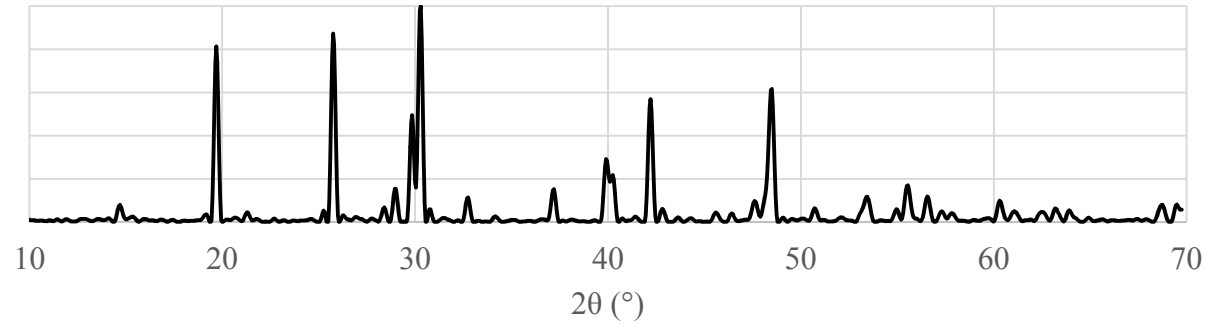

Figure S5. pXRD diffractogram of $LaBSiO_5$. All observed peaks are from $LaBSiO_5$ (PDF 50-237).

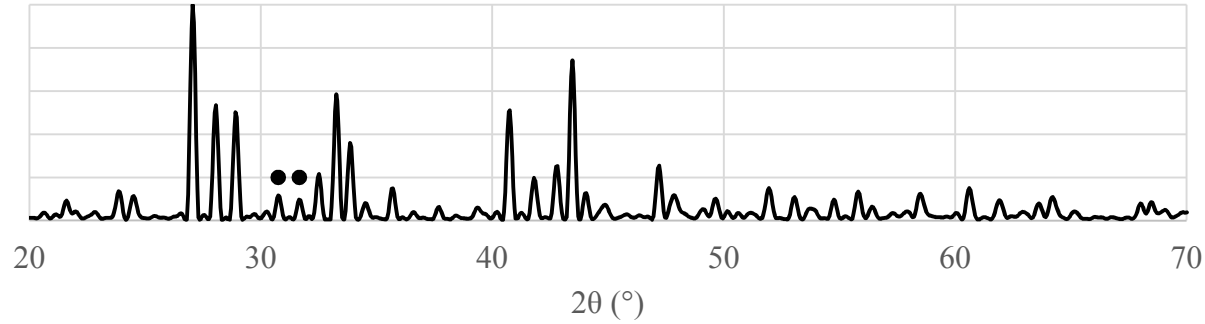

Figure S6. pXRD diffractogram of $La_2(SO_4)_3 \cdot 9H_2O$ (PDF 89-6401). Circles (●) indicate peaks from an unidentified impurity.

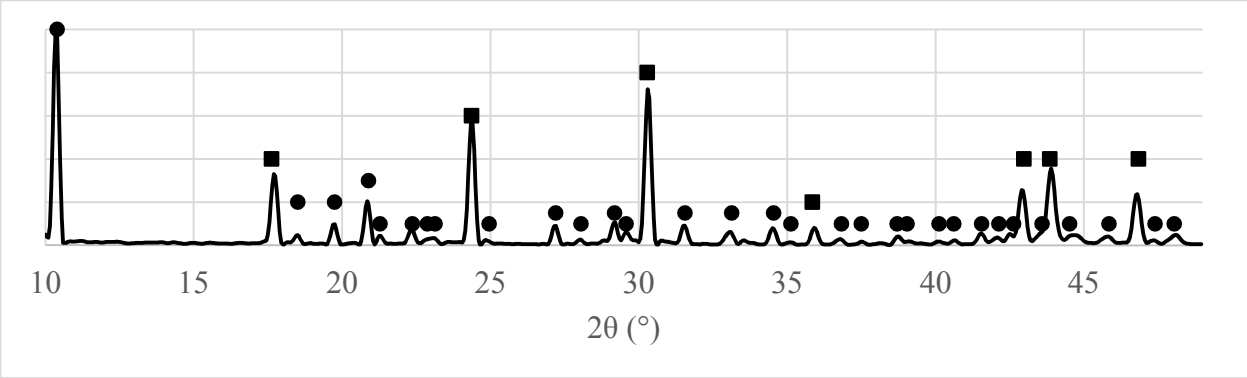

Figure S7. pXRD diffractogram of $La_2(CO_3)_3 \cdot 8H_2O$. Circles (●) indicate peaks from $La_2(CO_3)_3 \cdot 8H_2O$ (PDF 73-439). Squares (■) indicate peaks from $La(CO_3)(OH)$ (PDF 26-815).

Thermogravimetric Analysis

TGA was carried out using an aluminum crucible in a NETSZCH TG 209 F3 instrument under nitrogen atmosphere. 33.05 mg of $LaPO_4 \cdot nH_2O$ was heated from room temperature to 500 °C based upon previous literature studies[1]. 31.71 mg of $La_2(SO_4)_3 \cdot nH_2O$ was heated from room temperature to 800 °C based upon previous literature studies.[2]

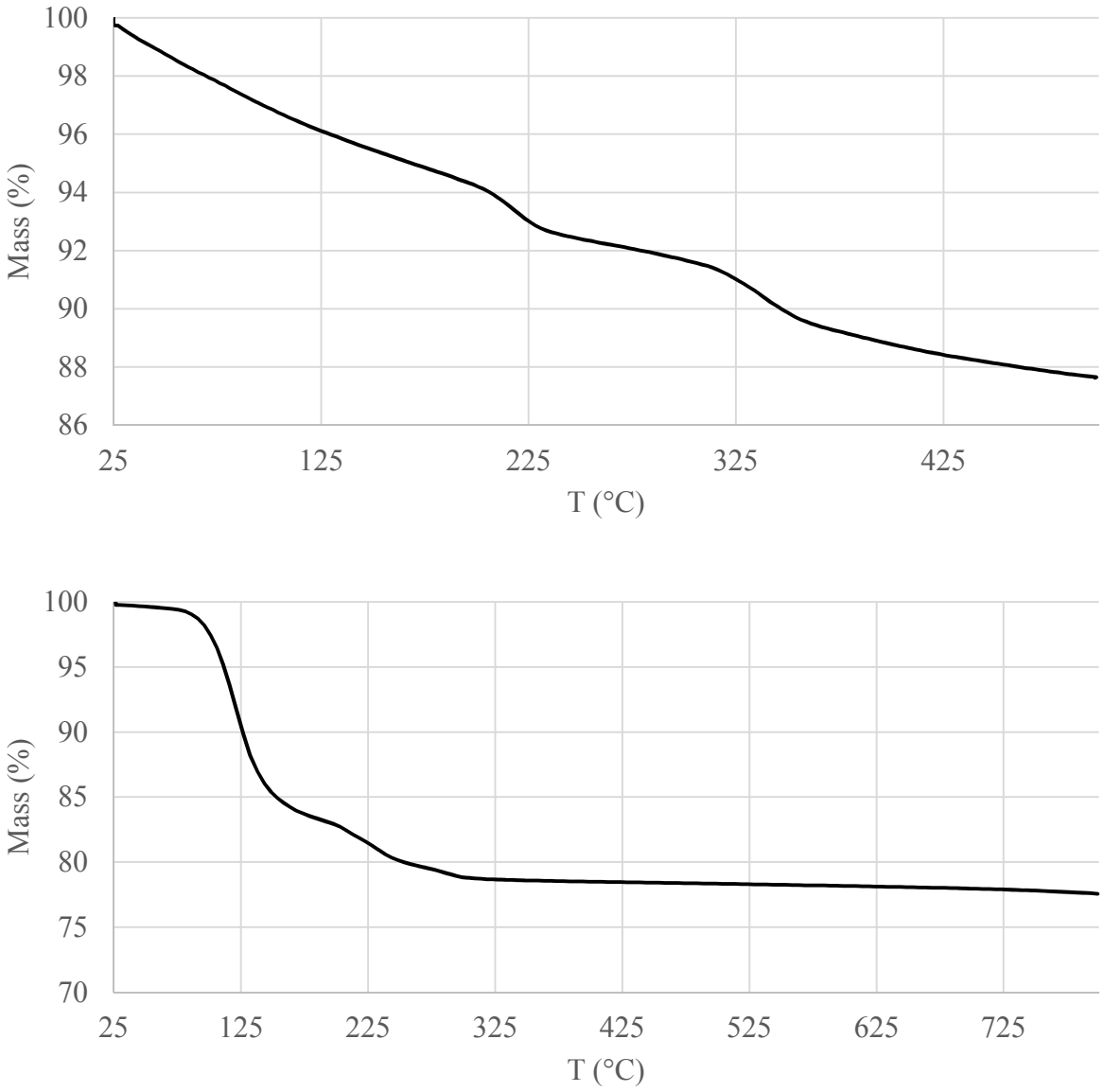

Figure S8. Top: TGA thermogram of $LaPO_4 \cdot nH_2O$. Bottom: TGA thermogram of $La_2(SO_4)_3 \cdot nH_2O$.

Based upon these plots (with 12.37% and 22.44% mass loss, respectively), we calculate *n* of $LaPO_4 \cdot nH_2O$ to be 1.84, and *n* of $La_2(SO_4)_3 \cdot nH_2O$ to be 9.08.

Density Functional Theory Calculations

Table S1. Atomic parameters used in this study. The electron valence of each atom is given, along with the configuration of the PAW projectors. The PAW radius is provided in atomic units. All nuclear quadrupole moment were taken from the literature[3]. Any atom not mentioned here was taken without alteration from the JTH PAW dataset table.

Atom	Valence	Projected	Radius	q_{zz} (bn)
H	$1s^1$	3*s*	0.5	0
B	$2s^2 2p^1$	2*s*, 2*p*	1.2	0.04059
O	$2s^2 2p^4$	2*s*, 2*p*	1.3	-0.02558
Si	$3s^2 3p^2$	2*s*, 2*p*	1.55	0
P	$3s^2 3p^3$	2*s*, 2*p*	1.5	0
S	$3s^2 3p^4$	2*s*, 2*p*	1.45	-0.0678
Ge	$4s^2 4p^2$	2*s*, 2*p*, 1*d*	1.85	-0.196

Table S2. Specific details regarding the calculations performed in this study. Both the plane-wave cutoff and the PAW fine grid cutoff are in hartree. All calculations save $LaScO_3$ used shifted Monkhorst-Pack grids of the dimensions below; $LaScO_3$ and $LaNbO_4$ used grids not parallel to the reciprocal lattice vectors.

System	Plane-wave Cutoff	PAW Fine Grid	Grid	Grid Spacing ($Å^{-1}$)
La_2O_3	30	140	10x10x7	0.03
$LaPO_4 \cdot 0H_2O$	45	150	6x6x6	0.03
$LaPO_4$	45	150	4x4x5	0.04
$LaBO_3$	45	150	7x4x6	0.03
$LaBGeO_5$	45	105	6x6x6	0.02
$LaBSiO_5$	45	150	5x5x5	0.03
$La_2(SO_4)_3 \cdot 9H_2O$	25	75	3x3x4	0.03
$La(OH)_3$	40	150	7x7x12	0.02
$LaAlO_3$	35	110	8x8x8	0.02
$LaCoO_3$	40	150	9x9x9	0.02
$LaCrO_3$	45	150	6x6x4	0.03
$LaScO_3$	20	40	0 5 3 5 0 3 5 5 0	0.03
$LaNbO_4$	30	90	-4 0 4 -4 -8 12 4 4 -4	0.04

Lanthanum Oxide

La_2O_3 has been previously investigated by ^{139}La ssNMR: first by Bastow in 1994, using a frequency-swept spin-echo technique;[4] and more recently by Spencer et al. using a WURST echo.[5] Given the thorough understanding of La_2O_3 in the literature, it is a good choice as a test compound for the implementation of WCPMG and VOCS, as well as for validating computational methods. La_2O_3 crystals are hexagonal and of space group P-3m1 with 1 formula unit per unit cell.[6] The lanthanum environment in La_2O_3 is the simplest of all of the compounds investigated in this work, described by Spencer et al. as "pseudo-octahedral". The LaO_7 coordination polyhedron is more precisely referred to as a face-capped octahedron, with two sets of three La-O bonds and the "cap" bond with lengths of 2.37 Å, 2.73 Å, and 2.46 Å respectively.

Our measured C_Q for La_2O_3 is 58.6 ± 0.3 MHz with an η of 0.00 ± 0.03, shown in Figure S9, in excellent agreement with the most recent literature values as reported by Spencer et al.[5] We used the same CSA values as Spencer et al. in fitting both our 9.4 T and 16.4 T (Figure S10) spectra to good effect.

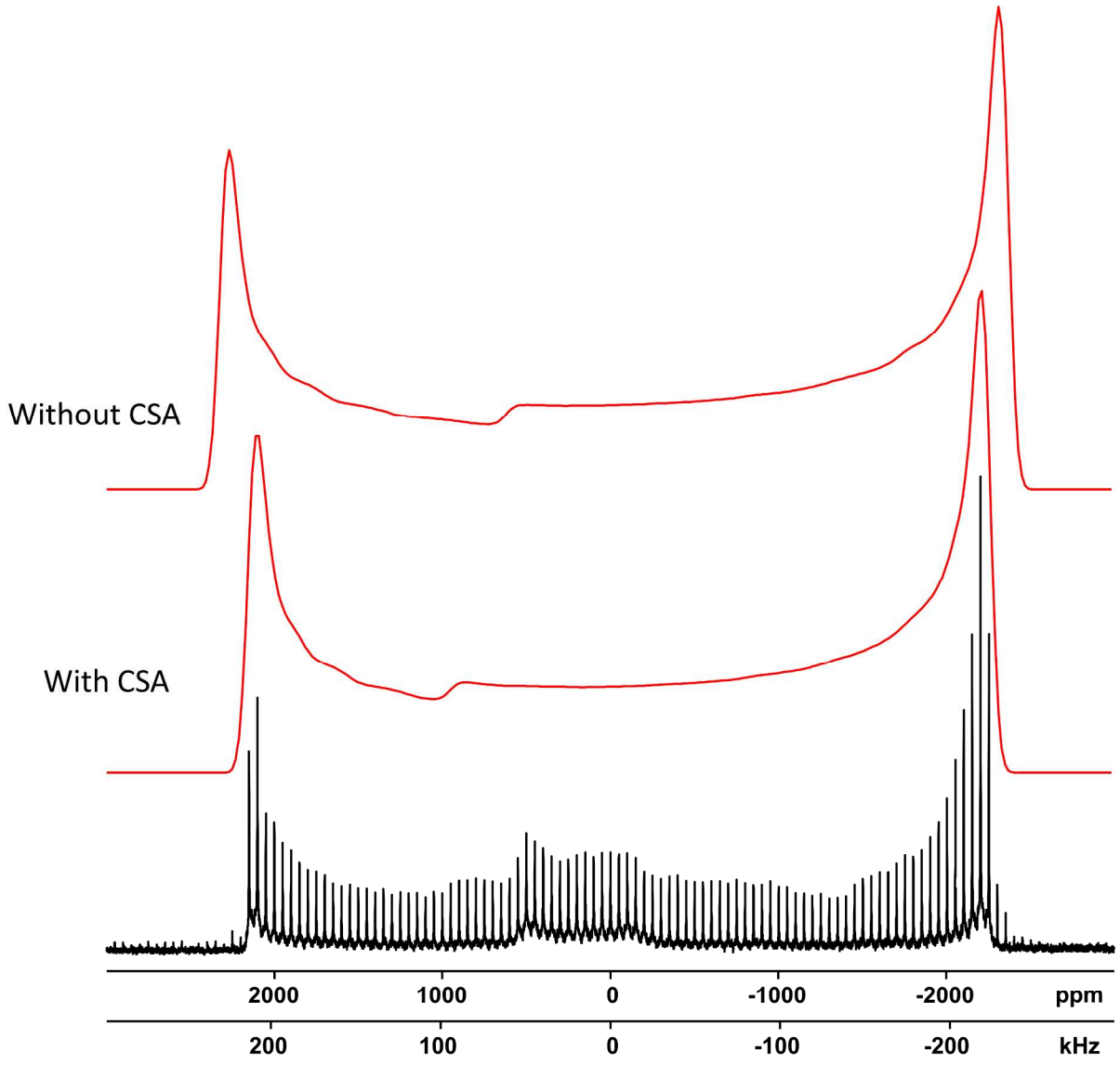

Figure S9. Static ^{139}La NMR spectrum of La_2O_3. Analytical simulation is show in red. The EFG and CSA parameters used are given in Table 1 in the main text.

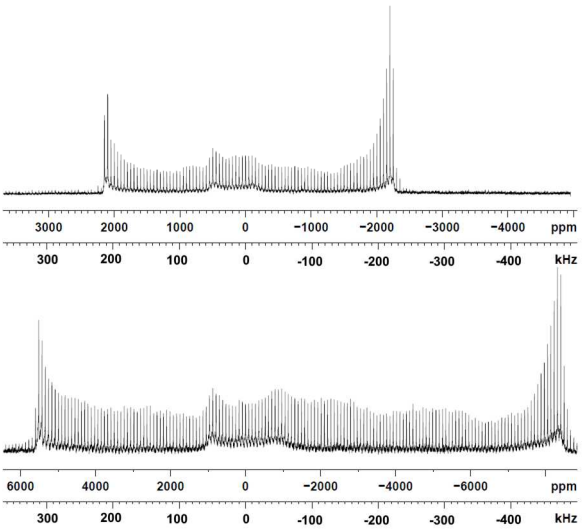

Figure S10. Static ^{139}La NMR spectra of La_2O_3. Both spectra are set to the same frequency scale. Top: Spectrum collected at 16.4 T. Bottom: Spectrum collected at 9.4 T.

DFT calculations of the EFG at the La^{3+} site using the experimental geometry[6] yielded a C_Q of 60.5 and an η of 0.0, which is in good agreement with the experimental results. When examining the calculated EFG tensor, the largest component V_{zz} is aligned with the La-O bond of the cap oxygen, and is parallel to the c-axis of the unit cell as shown in Figure S11. The c-axis in La_2O_3 possesses threefold rotational symmetry, which is consistent with both the observed and calculated η of 0.

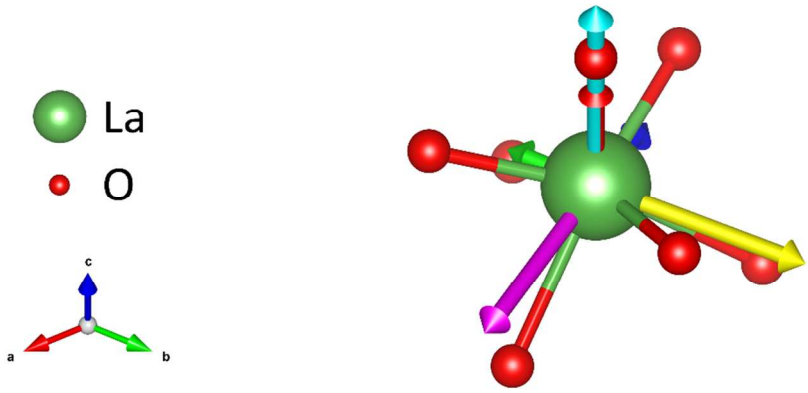

Figure S11. First coordination sphere of LaO_7 in La_2O_3. The V_{xx}, V_{yy}, and V_{zz} components are displayed as blue, green, and red, respectively. The e_a, e_b, and e_c semi major axes are in yellow, magenta, and teal respectively.

The least-squares ellipsoid that is fit to the LaO_7 polyhedron in La_2O_3 is a prolate spheroid, with semi major axes $e_a = e_b = 2.481 \pm 0.002$ Å and $e_c = 2.731 \pm 0.002$ Å and ellipsoid character of 1.00 ± 0.01. There is a moderate departure from spherical symmetry, with $\epsilon = 0.098 \pm 0.002$. The ellipsoid is aligned with the EFG tensor, with the largest semi major axis e_c parallel with V_{zz}, and the two other semi major axes in the plane defined by V_{xx} and V_{yy}, perpendicular to V_{zz}.

Lanthanum Phosphate Hydrate

$LaPO_4 \cdot nH_2O$, also known as rhabdophane, is a rare-earth phosphate mineral that has been proposed for use in environmental phosphate sequestration.[7] The structure of rhabdophane was first proposed by Mooney in 1950.[8] Rhabdophane is reported to be of the hexagonal $P6_222$ space group, with zeolitic channels parallel to the c axis and 3 formula units per cell. The lanthanum environment is eightfold coordinate to oxygen, with bond lengths reported: four bonds of length 2.34 Å and four of length 2.66 Å. The reported bond lengths, however, do not include any possible zeolitic water contributions. There are no obvious symmetry elements in the LaO_8 polyhedron that would force a particular value of η.

The sample of $LaPO_4 \cdot nH_2O$ used was determined to be $LaPO_4 \cdot 1.8H_2O$ through the use of TGA (Figure S8). Our ^{139}La NMR spectrum of this sample is fit using a C_Q of 33 ± 1 MHz with an η of 1.00 ± 0.05 (Figure S12). This conflicts with the spectrum reported by Dithmer et al.,[7] where they observed a broad, largely featureless resonance. The difference may result from different methods of preparation, resulting in dramatically differing crystallinity.

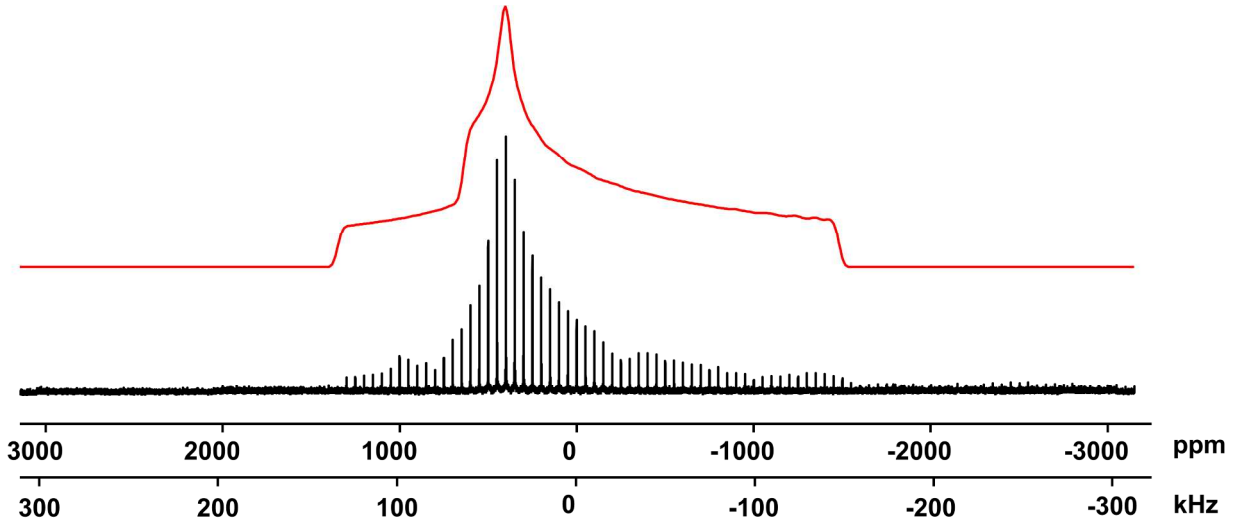

Figure S12. Static ^{139}La NMR spectrum of $LaPO_4 \cdot 1.8H_2O$. Analytical simulation is show in red. The EFG and CSA parameters used are reported in Table 1 in the main text.

The DFT calculations conducted on the experimental geometry provided by Mooney[8] yield a C_Q of -136 MHz and an η of 0.5, which is significantly at odds with the experimental results. While the difference can be explained in part by the absence of zeolitic water in the structure used for the calculation, it is unlikely for a small amount of water to cause such a large

disparity in C_Q. It has been suggested by Mesbah et al. that the structure of $LnPO_4 \cdot nH_2O$, including $LaPO_4 \cdot nH_2O$, is in fact monoclinic.[9] However, the structure proposed by Mesbah et al. contains six unique lanthanide sites, which are not resolved in the spectrum of $LaPO_4 \cdot 1.8H_2O$. Due to the extreme difference between experimental and calculated results, we place little stock in the orientation of the EFG tensor determined through our DFT calculations.

The LaO_8 polyhedron in $LaPO_4 \cdot nH_2O$ as reported by Moody is poorly fit by either a sphere or an ellipsoid, and as such is not included in any structural models.

Lanthanum Phosphate

Anhydrous $LaPO_4$ is better known as the mineral monazite.[10] Monazite was historically a commercial source of lanthanides, but it fell into disuse in part due to the presence of the radioactive daughter ions of thorium. The lanthanum environment in $LaPO_4$ is more complicated than the hydrated equivalent: the lanthanum site is ninefold coordinate, with significant variation in bond lengths. La-O bond lengths range from 2.47 Å to 2.78 Å, with an average bond length of 2.58 Å.

The experimental ^{139}La ssNMR spectrum of $LaPO_4$ is presented in Figure S13. The spectrum was fit using two sites: one site with a C_Q of 46.7 ± 1 MHz and an η of 0.75 ± 0.05, which is consistent with the values reported by Dithmer et al.;[7] and one using the parameters reported above for $LaPO_4 \cdot 1.8H_2O$. The sample appears to have undergone hydration between heating and collection of the spectrum. There is no appreciable CSA contribution visible in the lineshape at 16.4 T.

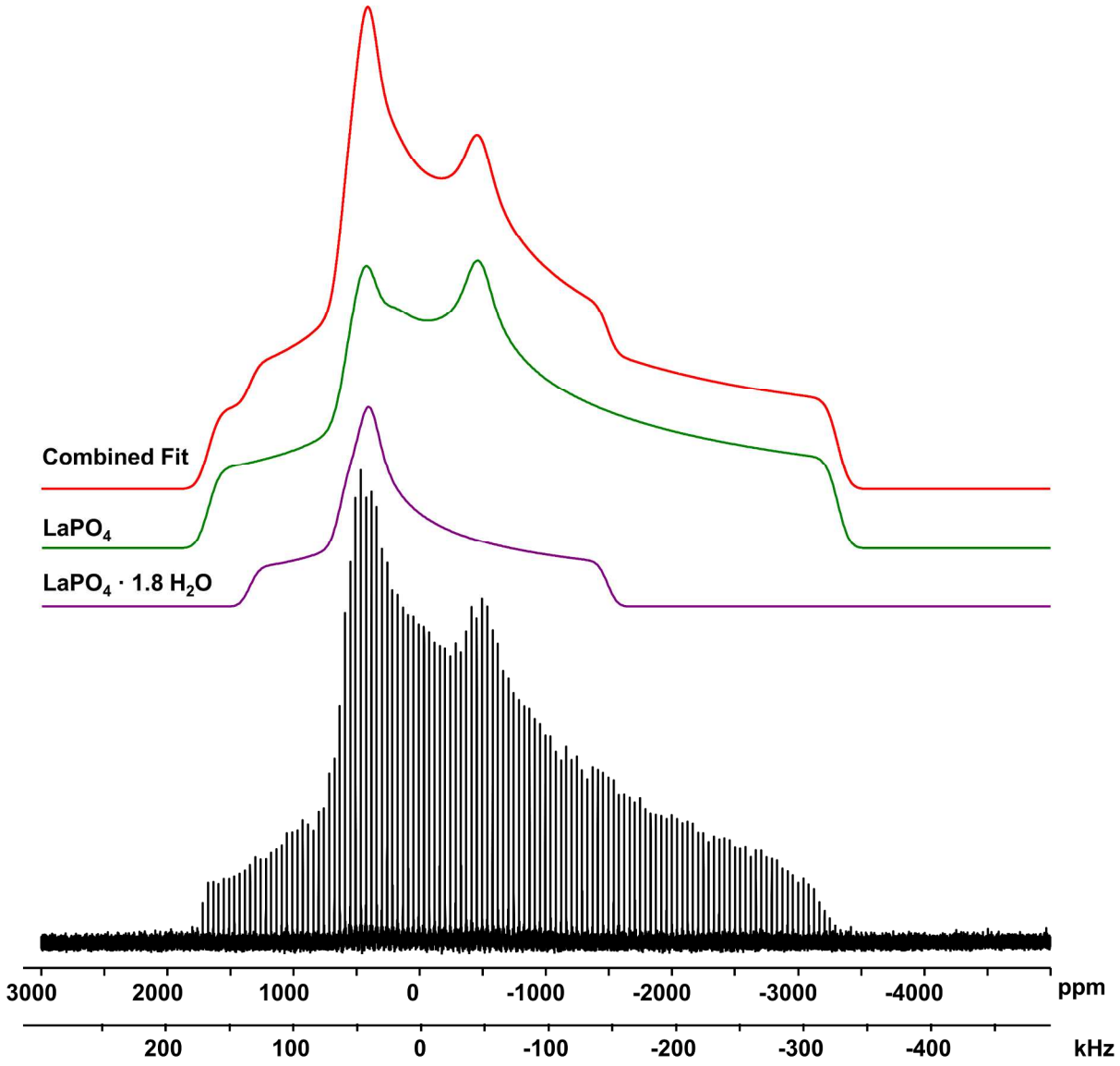

Figure S13. Static ^{139}La NMR spectrum of $LaPO_4$. Total analytical simulation is show in red. The simulations of the individual sites are in green ($LaPO_4$) and purple ($LaPO_4 \cdot 1.8H_2O$). The EFG and CSA parameters used are reported in Table 1 in the main text.

DFT calculations of $LaPO_4$ using the experimental geometry[10] yield a C_Q of 53.6 MHz and an η of 0.56. The calculations somewhat overestimates C_Q and underestimates η, but are consistent with the experimental results. Both the higher C_Q and lower η than experiment can both be explained by an overestimation of V_{zz} in the theoretical results. None of the tensor components are oriented toward any particular feature of the LaO_9 polyhedron.

The ellipsoid fitting the LaO_9 polyhedron is triaxial in nature, with $e_a = 2.415 \pm 0.001$ Å, $e_b = 2.574 \pm 0.001$ Å, and $e_c = 2.796 \pm 0.001$ Å. There is significant deviation from spherical symmetry, with $\epsilon = 0.147 \pm 0.001$ and a character of 0.05 ± 0.01. The V_{zz} component is nearest to the e_c axis, but the EFG tensor is generally not aligned with the ellipsoid of best fit (Figure S14).

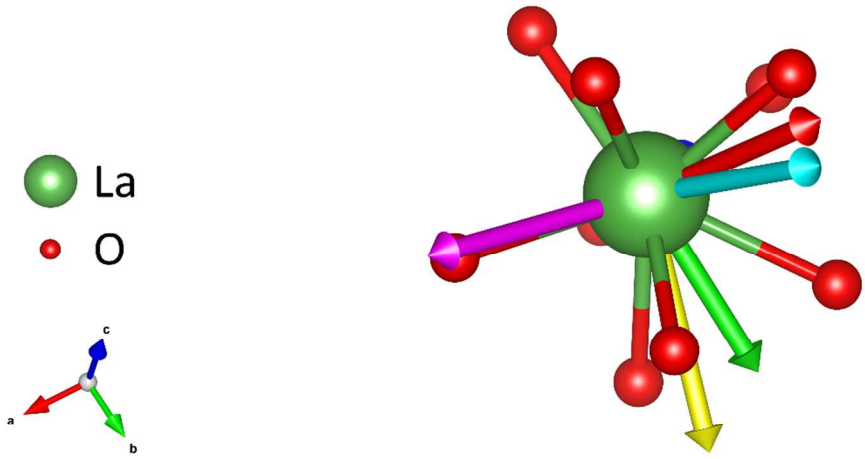

Figure S14. First coordination sphere of LaO_9 in $LaPO_4$. The V_{xx}, V_{yy}, and V_{zz} components are displayed as blue, green, and red, respectively. The e_a, e_b, and e_c semi major axes are in yellow, magenta, and teal respectively.

Lanthanum Borate

$LaBO_3$ has previously been investigated using ^{11}B ssNMR by Kroeker and Stebbins,[11] but has not been probed by ^{139}La ssNMR. $LaBO_3$ is a possible side product in the synthesis of $LaBGeO_5$ and $LaBSiO_5$,[12] as well as the primary phase to crystallize out of La_2O_3-B_2O_3 glasses. The room temperature phase of $LaBO_3$ is orthorhombic, with space group Pnma and 4 formula units per cell[13]. The lanthanum environment is ninefold coordinate to oxygen, with four La-O bond pairs of lengths 2.41 Å, 2.49 Å, 2.77 Å, and 2.80 Å, and one La-O bond of length 2.38 Å. The average La-O bond length is 2.59 Å. There is a mirror plane bisecting the LaO_9 polyhedron, with the independent La-O bond parallel to the plane.

Using the ^{139}La ssNMR spectra of $LaBO_3$ measured at 9.4 T and 16.4 T (Figure S15, Figure S16), the quadrupole and chemical shift parameters could be determined. The quadrupole coupling has a value of C_Q of 23.4 ± 0.4 MHz with an η of 0.68 ± 0.05. There is a significant CSA contribution to the lineshape, with Ω = 350 ± 30 ppm, κ = 0.3 ± 0.1, and Euler angles α = 15 ± 5°, β = 0 ± 5°, and γ = 165 ± 10°. The magnitude of the CSA parameters is significant when compared to the quadrupolar influence on the lineshape: the measured span for the La^{3+} site of $LaBO_3$ is comparable to La_2O_3 or $LaScO_3$, while the ^{139}La C_Q of La^{3+} in $LaBO_3$ is significantly less than that in La_2O_3 or $LaScO_3$.

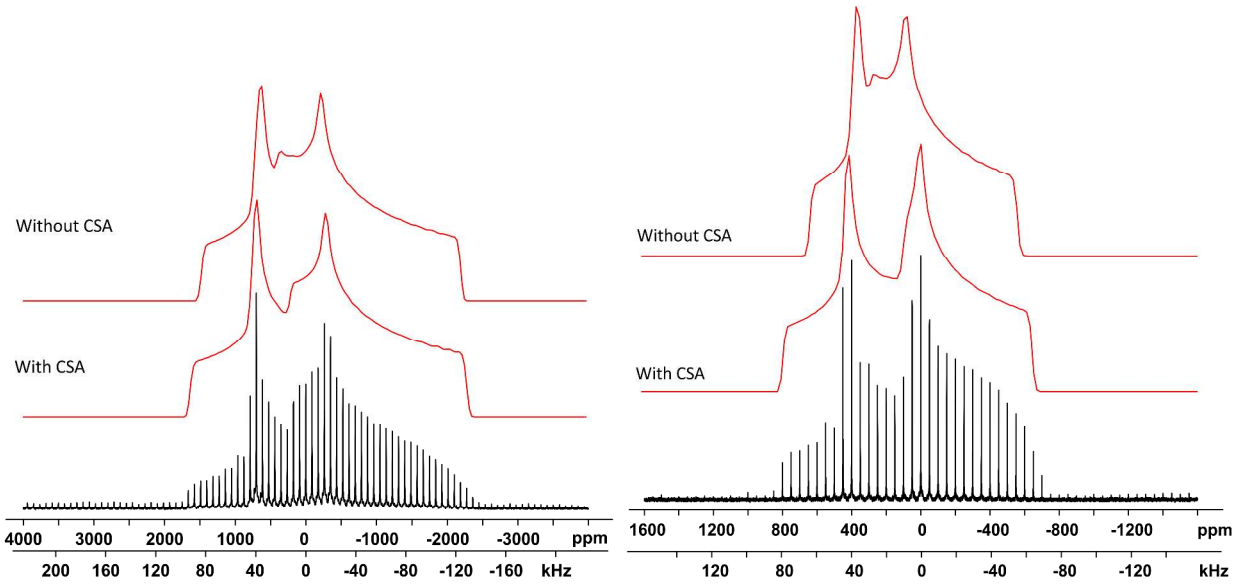

Figure S15. Static ^{139}La NMR spectra of $LaBO_3$. Analytical simulations are shown in red. The EFG and CSA parameters used are reported in Table 1 in the main text. Left: Spectrum collected at 9.4 T. Right: Spectrum collected at 16.4 T.

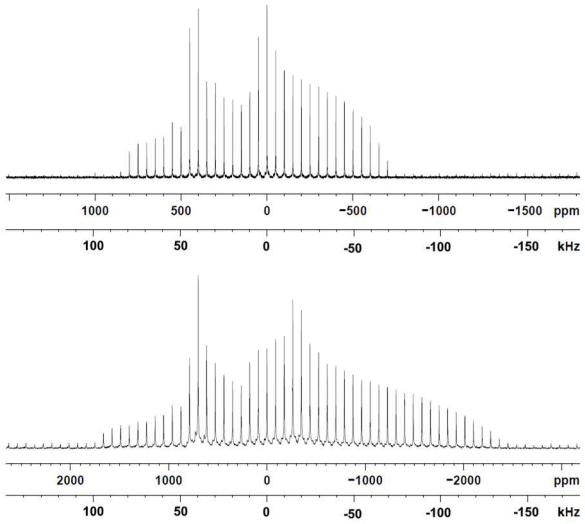

Figure S16. Static ^{139}La NMR spectra of $LaBO_3$. Both spectra are set to the same frequency scale. Top: Spectrum collected at 16.4 T. Bottom: Spectrum collected at 9.4 T.

DFT calculations of $LaBO_3$ on the experimental geometry[13] yielded a C_Q of -28.8 MHz with an η of 0.57. Both values agree reasonably well with experiment, though the C_Q is overestimated. Calculations carried out on a different $LaBO_3$ structure[14] using the same parameters reported a C_Q of -84 and η of 0.05, which are even further from experiment. The ^{139}La C_Q of $LaBO_3$ appears to be extremely sensitive to structure, which should be considered when comparing experimental and computational values.

The least-squares ellipsoid which fits the LaO_9 polyhedron in $LaBO_3$ is significantly distorted, with $\epsilon = 0.157 \pm 0.001$ and semi major axes $e_a = 2.331 \pm 0.001$ Å, $e_b = 2.721 \pm 0.001$

Å, and e_c = 2.741 ± 0.001 Å. The character is nearly wholly oblate at -0.92 ± 0.01. This is at odds with the experimental η, as a small value of η would be expected when the system is nearly axially symmetric. The V_{xx} EFG component is antiparallel to the e_b semi major axis, and the V_{zz} component is close to the e_a axis.

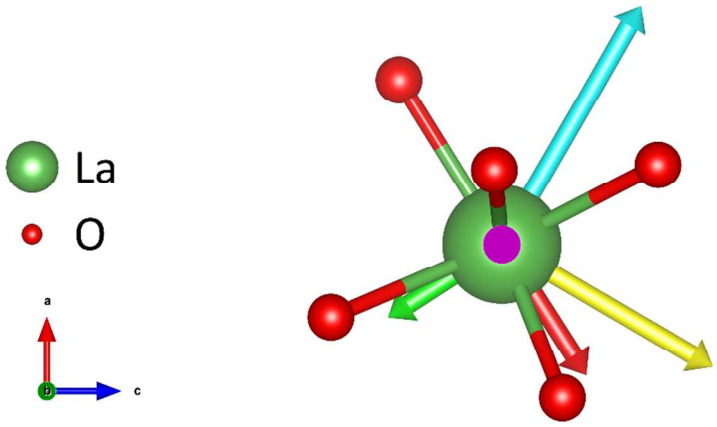

Figure S17. First coordination sphere of LaO_9 in $LaBO_3$. The V_{xx}, V_{yy}, and V_{zz} components are displayed as blue, green, and red, respectively. The e_a, e_b, and e_c semi major axes are in yellow, magenta, and teal respectively.

Lanthanum Borosilicate

Another member of the stillwellite family, $LaBSiO_5$ (LBS) is the silicate analogue of LBG, and is isostructural to LBG.[15] Also of space group $P3_1$, the lanthanum environment of LBS is of slightly higher coordination, forming a LaO_{10} polyhedron. This difference is attributed to the difference in size between the GeO_4 and SiO_4 tetrahedra[16]. La-O bonds range in length from 2.39 Å to 2.86 Å, with an average of 2.64 Å. Like LBG, there are no obvious symmetry elements present in the lanthanum polyhedron of LBS.

The ^{139}La ssNMR spectrum of LBS is presented in Figure S18. The lineshape is fit with a C_Q of 90 ± 0.5 MHz and η of 0.35 ± 0.02. The spectrum of LBS is the broadest presented in this study, and among the broadest reported in the literature.[17] While similar in shape to the spectrum of LBG, the spectrum of LBS is slightly broader and slightly less axially symmetric, likely a consequence of the higher coordination number.

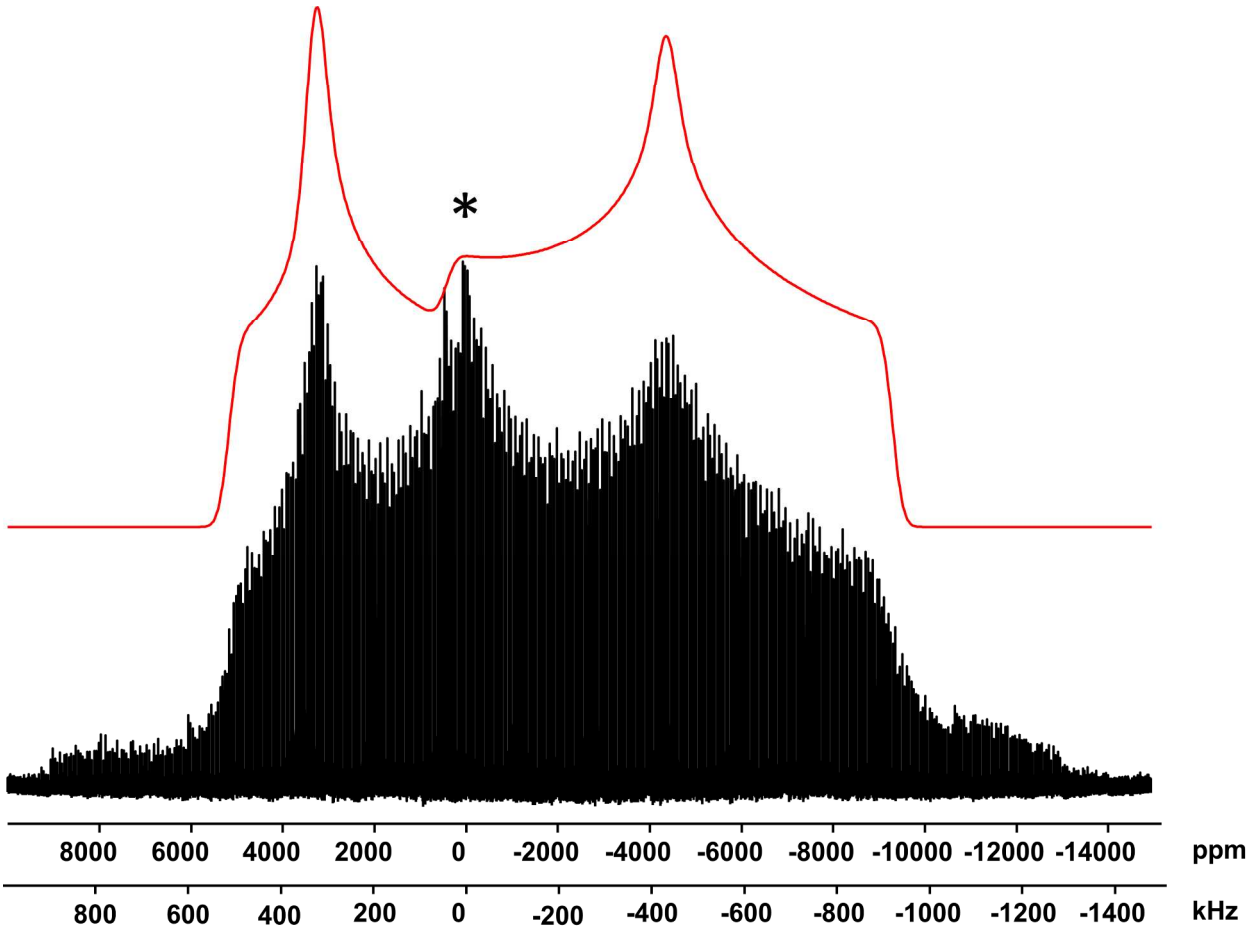

Figure S18. Static ^{139}La NMR spectrum of $LaBSiO_5$. Analytical simulation is show in red. The EFG parameters used are reported in Table 1 in the main text. The presence of an impurity is indicated with an asterisk.

The DFT calculations on LBS produce results which vary significantly from experiment. The theoretical calculations on the experimental geometry[15] yield a ^{139}La C_Q of -110 MHz and η of 0.05, neither of which are consistent with the experimental results. Given the apparent sensitivity of $LaBO_3$ and $LaScO_3$ to small changes in geometry, agreement with experiment could be improved by using a different experimental structure.

The coordination ellipsoid of lanthanum in LBS is quite oblate, with e_a = 2.350 ± 0.001 Å, e_b = 2.713 ± 0.001 Å, e_c = 2.808 ± 0.001 Å, leading to a character of with a character of -0.67, but is less so than that of LBG. The span of this ellipsoid is quite large at 0.175. The semi major axis e_b is very nearly aligned with the V_{yy} EFG component, and the V_{zz} EFG component is close to the e_a axis (Figure S19).

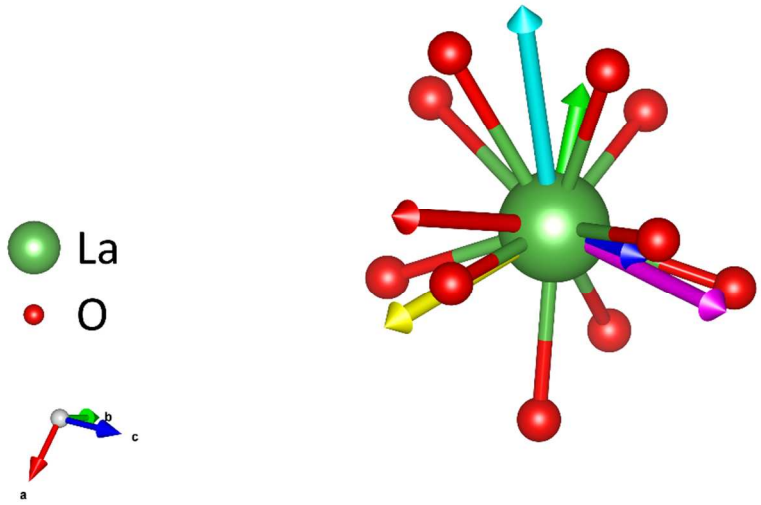

Figure S19. First coordination sphere of LaO_{10} in $LaBSiO_5$. The V_{xx}, V_{yy}, and V_{zz} components are displayed as blue, green, and red, respectively. The e_a, e_b, and e_c semi major axes are in yellow, magenta, and teal respectively.

Lanthanum Sulfate Nonahydrate

$La_2(SO_4)_3 \cdot 9H_2O$ is a commercially available lanthanum compound with a defined crystal structure, making it a good model compound for this investigation. $La_2(SO_4)_3 \cdot 9H_2O$ is of the hexagonal $P6_3/m$ space group with two formula units per unit cell.[18] There are two lanthanum sites in $La_2(SO_4)_3 \cdot 9H_2O$: site La(1), with twelvefold coordination; and site La(2), with ninefold coordination. Both sites have highly symmetric polyhedra with C_3 rotation axes parallel to the crystallographic c axis. La(1) is best described as a distorted LaO_{12} icosahedron, and La(2) as a LaO_9 tricapped trigonal prism. As a result, both sites are predicted to have η values of 0, but will have non-zero C_Q values. La(1) has two sets of bonds: three pairs of La-O bond length 2.59 Å, and three pairs of length 2.80 Å, with an average length of 2.70 Å. La(2) has two different bond lengths: the equatorial La-O bonds of length 2.51 Å, and the non-equatorial bonds of length 2.55 Å. The second coordination sphere of the two sites also has significant variation. The La(1) icosahedron edge-shares with six SO_4 tetrahedra, where the La(2) site corner-shares with three sulfur tetrahedra which cap the rectangular faces of a trigonal prism. This trigonal prism is formed by water oxygen coordinating to lanthanum. La(1) has no H_2O in its near proximity, whereas the environment of La(2) is dominated by it.

The difference in the local structure of the two sites is reflected in the spectrum of $La_2(SO_4)_3 \cdot 9H_2O$ (Figure S20). Two peaks are observed: peak 1, with isotropic chemical shift $\delta_{iso} = -175 \pm 25$ ppm, $C_Q = 52.5 \pm 0.5$ MHz, and $\eta = 0.00 \pm 0.02$; and peak 2, with $\delta_{iso} = -75 \pm 25$ ppm, $C_Q = 36.5 \pm 0.5$ MHz, and $\eta = 0.00 \pm 0.03$. Peak 1 is assigned to La(1) and peak 2 to La(2) based upon the computational results discussed below.

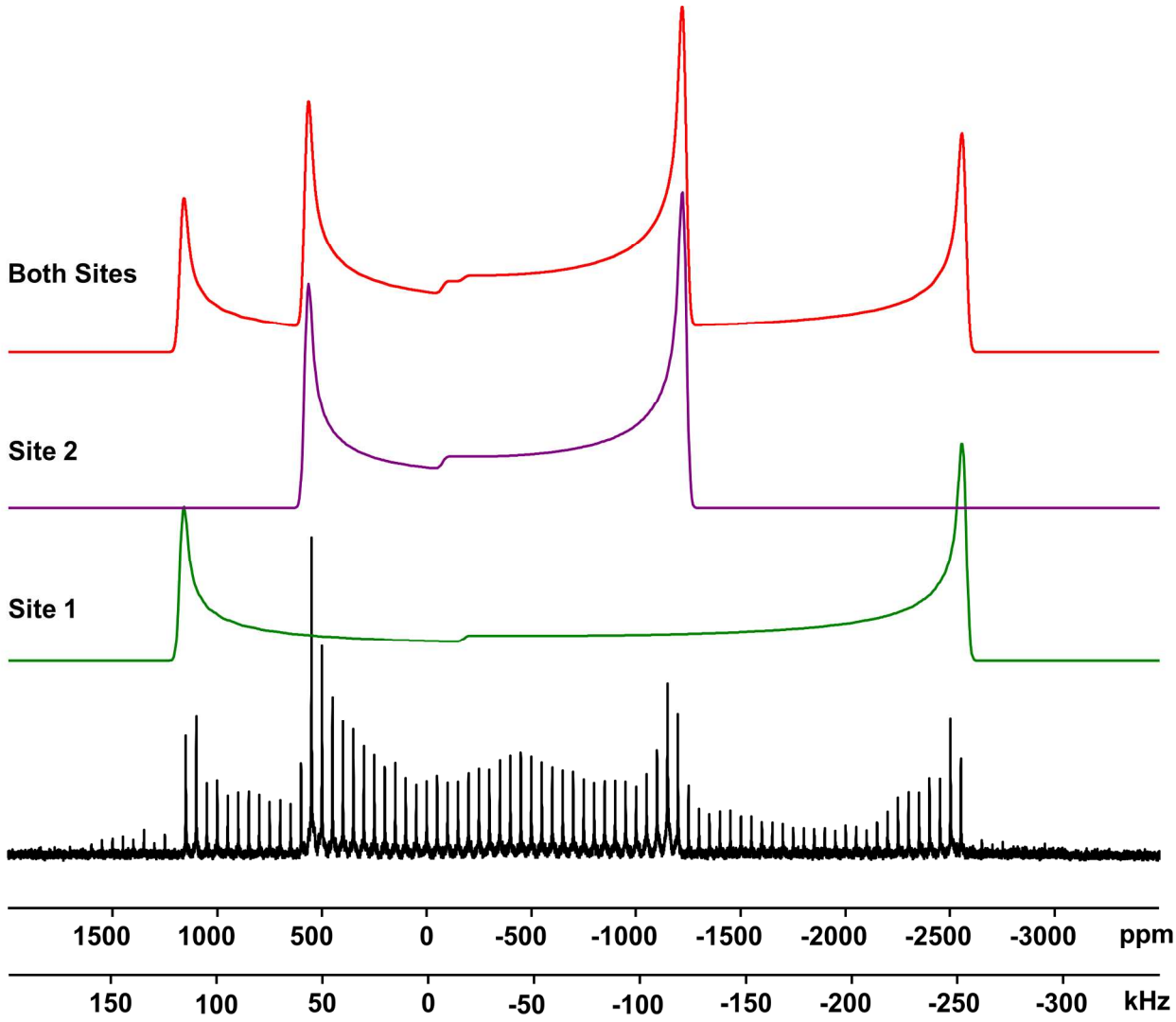

Figure S20. Static ^{139}La NMR spectrum of $La_2(SO_4)_3 \cdot 9H_2O$. Analytical simulation is show in red. The EFG parameters used are reported in Table 1 in the main text.

DFT calculations were based on the experimental geometry[18] of $La_2(SO_4)_3 \cdot 9H_2O$, but there are no experimentally reported values for the position of the hydrogen atoms. We manually placed hydrogen atoms at reasonable starting locations and optimized their positions, holding the position of all other atoms (i.e. La, S, and O) constant. Our calculations yield a C_Q of -59.1 MHz and η of 0.0 for La(1) and C_Q of -36.5 MHz and η of 0.0 for La(2). The asymmetry parameters are confined by symmetry, but the magnitudes of the quadrupolar coupling constants agree reasonably well with the fit proposed above. The difference in the calculated C_Q of the two sites is used as a basis for assigning peak 1 to site La(1) and peak 2 to site La(2). The V_{zz} component of the EFG at La(1) is collinear to the crystallographic c axis, and as such is directed towards the neighbouring LaO_{12} icosahedron. In site 2, V_{zz} is also collinear to the crystallographic c axis, with V_{xx} and V_{yy} consequentially in the crystallographic a-b plane.

Both sites can be fit independently by least-squares ellipsoids. Both are spheroids, as expected due to their axial symmetry. The ellipsoid of La(1) is oblate, with e_a = 2.463 ± 0.001 Å and $e_b = e_c$ = 2.837 ± 0.001 Å. Despite the icosahedral nature of the LaO_{12} polyhedron, there is significant distortion from spherical symmetry with ϵ = 0.138 ± 0.001. The character of the ellipsoid is -1.00 ± 0.01, as expected from an oblate spheroid. Considering the LaO_{12} ellipsoid, the shortest semi-major axis is aligned with the crystallographic c axis, and hence collinear with V_{zz}. The ellipsoid of La(2) is prolate, with $e_a = e_b$ = 2.514 ± 0.001 Å and e_c = 2.585 ± 0.001 Å. The La(2) ellipsoid is significantly less distorted than the La(1) ellipsoid, with ϵ = 0.028 ± 0.001. As a prolate spheroid, the character of the ellipsoid is 1.00 ± 0.01. The largest semi major axis is parallel to both V_{zz} and the crystallographic c axis. As a spheroid, the direction of the degenerate semi major axes is not unique, and like V_{xx} and V_{yy} they also lies in the a-b plane (Figure S21).

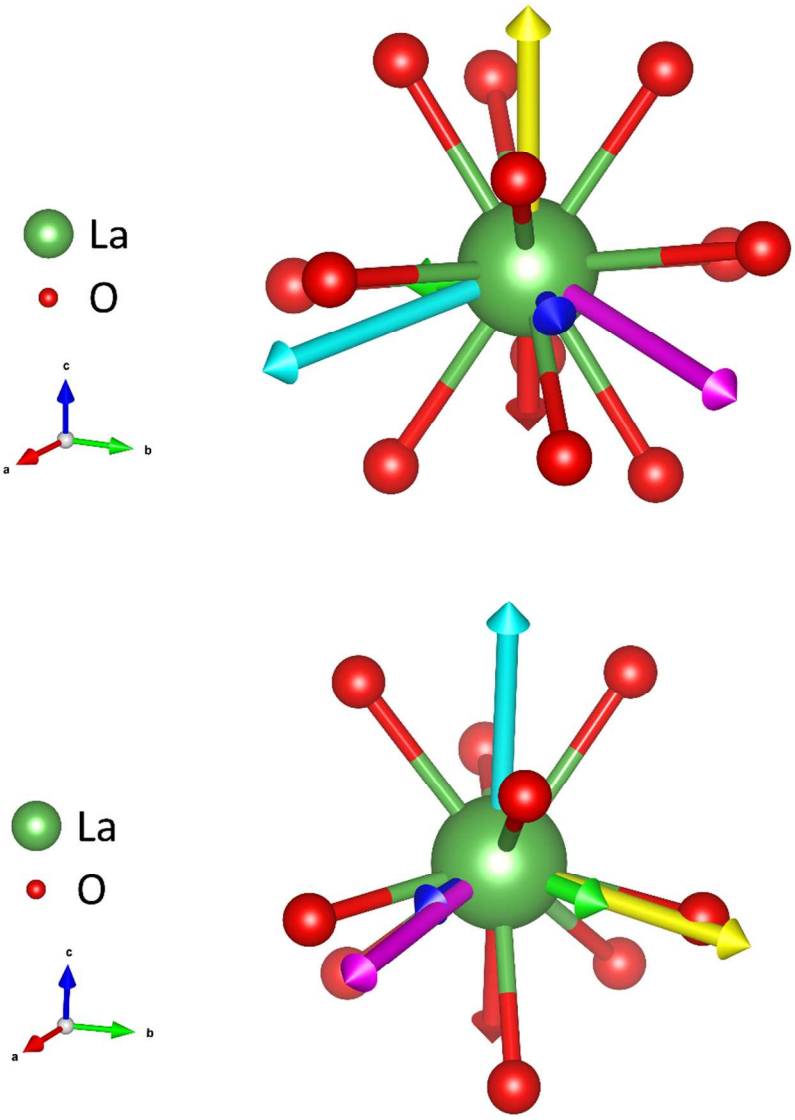

Figure S21. Top: First coordination sphere of LaO_{12} in $La_2(SO_4)_3 \cdot 9H_2O$. Bottom: First coordination sphere of LaO_9 in $La_2(SO_4)_3 \cdot 9H_2O$. The V_{xx}, V_{yy}, and V_{zz} components are displayed as blue, green, and red, respectively. The e_a, e_b, and e_c semi major axes are in yellow, magenta, and teal respectively.

Lanthanum Carbonate Octahydrate

Despite pXRD suggesting a crystalline sample of $La_2(CO_3)_3 \cdot nH_2O$, it was not possible to obtain a spectrum with sufficient resolution to separate the multiple sites present. The collected spectrum, presented in Figure S22, is believed to be a combination of the two sites[19] of $La_2(CO_3)_3 \cdot 8H_2O$ and the three sites[20] of lanthanum carbonate oxide ($LaCO_3OH$), the presence of which is suggested by pXRD (Figure S7).

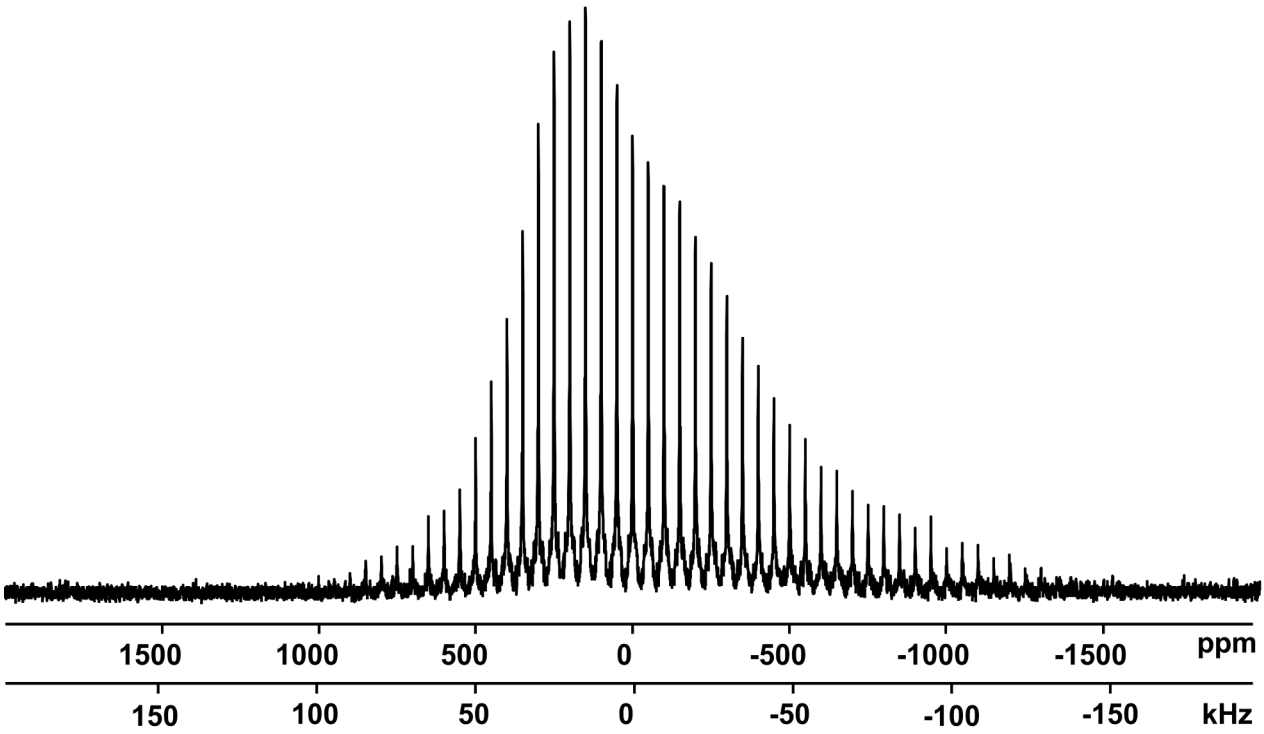

Figure S22. Static ^{139}La spectrum of sample of nominal composition $La_2(CO_3)_3 \cdot nH_2O$.

Given the multi-phase nature of the sample, along with the poor spectral resolution, DFT calculations on the lanthanum carbonate octahydrate system were not attempted.

Lanthanum Hydroxide

La_2O_3 will easily convert to $La(OH)_3$ under exposure to atmospheric water.[21] It has influenced previous ^{139}La NMR studies, and as a consequence has been well-studied using ^{139}La ssNMR[5]. We did not collect further spectra $La(OH)_3$ in this work.

$La(OH)_3$ is in the $P6_3/m$ space group, as confirmed by both X-ray and neutron diffraction studies.[22,23] The unit cell of $La(OH)_3$ contains two formula units. The lanthanum environment is ninefold coordinate, with only oxygen in the first coordination sphere. Like site La(2) of $La_2(SO_4)_3 \cdot 9H_2O$, the LaO_9 polyhedron in $La(OH)_3$ is a tricapped trigonal prism, with a threefold rotation axis parallel to the crystallographic c axis. This predicts an η of 0, which is confirmed by a previous study of $La(OH)_3$.[5]

We conducted DFT calculations on $La(OH)_3$ using the experimental geometry[23], with the positions of the hydrogen atoms determined through neutron powder diffraction. Our DFT calculations yield a C_Q of -29 and an η of 0.0, consistent with the experimental results reported by Spencer et al., who report an experimental C_Q of 22.0 ± 0.5 MHz and an η of 0.05 ± 0.02[5]. The V_{zz} component is collinear the crystallographic c axis, and is hence oriented to face the nearest neighbouring LaO_9 polyhedron.

The ellipsoid used to fit the LaO_9 polyhedron of $La(OH)_3$ is a prolate spheroid, with e_a = e_b = 2.551 ± 0.001 Å and e_c = 2.620 0.001 Å. It is very nearly spherical, with ϵ = 0.027 ± 0.01 and a character of 1.00 ± 0.01. The longest semi major axis is parallel to the crystallographic c axis and hence collinear with V_{zz} (Figure S23).

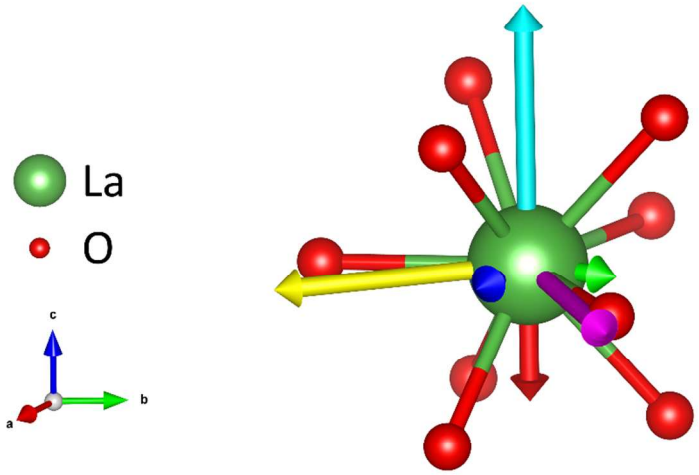

Figure S23. First coordination sphere of LaO_9 in $La(OH)_3$. The V_{xx}, V_{yy}, and V_{zz} components are displayed as blue, green, and red, respectively. The e_a, e_b, and e_c semi major axes are in yellow, magenta, and teal respectively.

Lanthanum Aluminate

$LaAlO_3$ is a rhombohedral perovskite of space group R -3 c with six formula units per unit cell. $LaAlO_3$ is remarkable in the NMR community for possessing one of the smallest reported ^{139}La C_Q values.[24] The coordination environment of lanthanum in $LaAlO_3$ is twelvefold coordinate, with the LaO_{12} polyhedron assuming a slightly distorted cuboctahedron geometry.[25] Despite the distortion, there is a C_3 rotation axis parallel to the crystallographic c axis, which enforces an η of 0.

The ^{139}La ssNMR spectrum of $LaAlO_3$ was first observed by Dupree et al., where they fit the lineshape with a C_Q of 6 MHz and an η of 0.[24] Given that the peak is narrow enough to be collected through magic angle spinning NMR, these values are quite reliable. We conducted DFT calculations on the experimental geometry,[25] which yielded a C_Q of 8.4 MHz and an η of

0.0. This is in good agreement with the experimental results of Dupree et al. The V_{zz} component of the EFG is parallel to the crystallographic c axis.

The ellipsoid of LaO_{12} in $LaAlO_3$ is the most spherical of all the compounds examined in this study, with $\epsilon = 0.01 \pm 0.01$. As is consistent with an η of 0, the ellipsoid is a spheroid; in particular it is an oblate spheroid, with $e_a = 2.67 \pm 0.01$ Å and $e_b = e_c = 2.70 \pm 0.01$ Å. The shortest semi major axis is parallel to both V_{zz} and the crystallographic c axis (Figure S24).

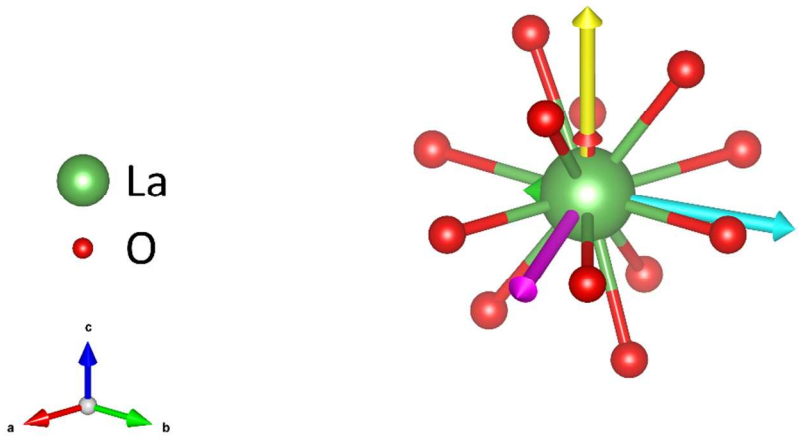

Figure S24. First coordination sphere of LaO_{12} in $LaAlO_3$. The V_{xx}, V_{yy}, and V_{zz} components are displayed as blue, green, and red, respectively. The e_a, e_b, and e_c semi major axes are in yellow, magenta, and teal respectively.

Lanthanum Cobaltite

$LaCoO_3$ is a member of the perovskite family, and is of the rhombohedral space group R -3 c with two formula units per cell.[26] $LaCoO_3$ has been previously studied using ^{139}La ssNMR by Bastow[4]. The lanthanum environment in $LaCoO_3$ is twelvefold coordinate to oxygen, forming a distorted cuboctahedron. There are three different La-O bond lengths in the LaO_{12} polyhedron: three of length 2.43 Å; six of length 2.69 Å; and three of length 2.99 Å; together with an average of 2.70 Å. There is a C_3 rotation axis parallel to the crystallographic c axis, enforcing an η of 0 on the lanthanum site.

Our DFT calculations of $LaCoO_3$ using the experimental geometry[26] yield a ^{139}La C_Q of 20.99 MHz and η of 0.00, in reasonable agreement with the experimental results of Bastow. Due to the resolution limits imposed by the frequency-stepped spin-echo technique used, Bastow estimated the C_Q to be 23.8 MHz by the separation of the satellite transitions, rather than by direct simulation of the central transition. V_{zz} is aligned with the C_3 rotation axis, and directed towards a face of a CoO_6 octahedron.

The ellipsoid fitting the LaO_{12} cuboctahedron is oblate and somewhat distorted, with $\epsilon = 0.04 \pm 0.03$ and a character of -1.00 ± 0.01. The semi major axes are $e_a = 2.67 \pm 0.04$ Å and $e_b = e_c = 2.78 \pm 0.04$ Å. As has been observed with other compounds fit by a spheroid, the non-degenerate semi major axis is parallel to the proper rotation axis of the polyhedron (Figure S25). The large uncertainty in the ellipsoid span indicates that the oxygen positions are not easily fit by

a triaxial ellipsoid; this is a consequence of the square (or in this distorted case, diamond) faces of the cuboctohedral geometry.

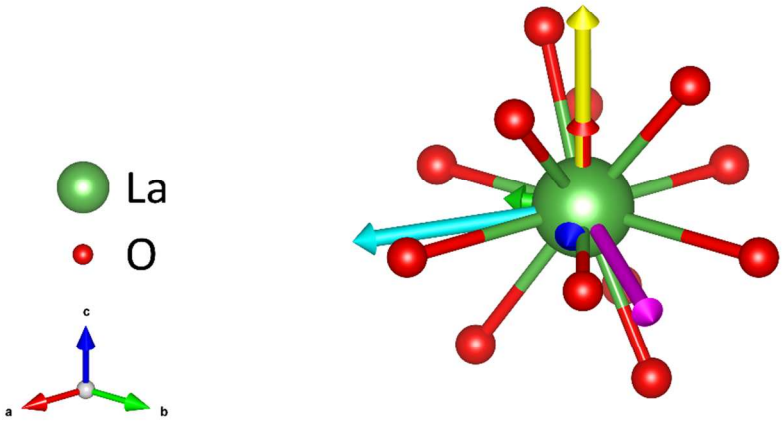

Figure S25. First coordination sphere of LaO_{12} in $LaCoO_3$. The V_{xx}, V_{yy}, and V_{zz} components are displayed as blue, green, and red, respectively. The e_a, e_b, and e_c semi major axes are in yellow, magenta, and teal respectively.

Lanthanum Chromite

At room temperature, $LaCrO_3$ is in the orthorhombic Pbnm space group with four formula units per cell.[27] It experiences an antiferromagnetic phase transition at approximately 286 K.[28] The lanthanum environment is twelvefold coordinate, forming a severely distorted LaO_{12} cuboctahedron. The distortion is sufficiently severe that there are no obvious symmetry elements prescribing particular NMR behavior. The La-O bond lengths in the LaO_{12} polyhedron range from 2.43 Å to 3.12 Å.

$LaCrO_3$ has been previously studied using ^{139}La ssNMR spectroscopy by Bastow, in which he fits the $LaCrO_3$ peak with a C_Q of 48 MHz and an η of 0.15.[4] Our DFT calculations on the experimental structure[27] yield a C_Q of -47.2 MHz with an η of 0.32. While the C_Q is in good agreement with experiment, our calculations overestimate the asymmetry parameter as reported by Bastow. However, given the relatively low resolution provided by the frequency-swept spin echo technique used, it is possible that the experimental η was underestimated. The V_{xx} axis is parallel to the crystallographic c axis, while the V_{yy} and V_{zz} components of neighbouring LaO_{12} polyhedra are nearly aligned (Figure S26).

The ellipsoid fitting the LaO_{12} cuboctahedron is triaxial, reflecting the level of distortion from spherical symmetry. The span is moderately high at $\epsilon = 0.16 \pm 0.05$, and the character of the ellipsoid is -0.14 ± 0.01, reflecting a slightly oblate nature. The semi major axis e_b is parallel to both the V_{xx} component and the crystallographic c axis, while V_{zz} is closely adjacent to e_a

(Figure S26). Like $LaCoO_3$, the coordination polyhedron is poorly fit by an ellipsoid; this is also attributed to the strongly distorted cuboctahedral geometry of the local lanthanum coordination.

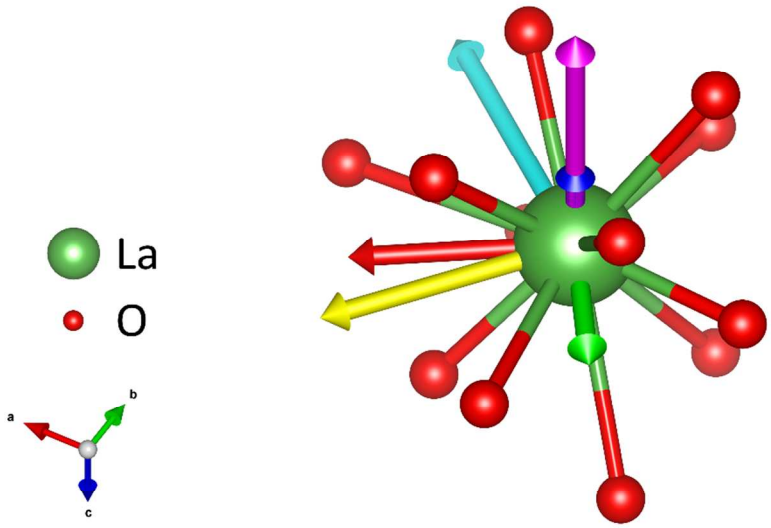

Figure S26. First coordination sphere of LaO_{12} in $LaCrO_3$. The V_{xx}, V_{yy}, and V_{zz} components are displayed as blue, green, and red, respectively. The e_a, e_b, and e_c semi major axes are in yellow, magenta, and teal respectively.

Lanthanum Titanate

$LaTiO_3$ has been studied for its role as an antiferromagnet,[29] as well as for its application in the battery material lithium lanthanum titanate.[30] $LaTiO_3$ is in the orthorhombic Pbnm space group with 4 formula units per unit cell. The lanthanum environment is eightfold coordinate in a distorted square antiprismatic configuration, with La-O bonds ranging from 2.43 Å to 2.77 Å, with an average of 2.60 Å. $LaTiO_3$ has been experimentally observed through low-temperature ^{139}La ssNMR by Furukawa et al. They reported a quadrupole resonance frequency of 3.8 MHz and an η of 0.6. [29] A ^{139}La quadrupole resonance frequency of 3.8 MHz is equivalent to a ^{139}La C_Q of 53.2 MHz. The value of η remains unchanged. The measurement of the quadrupolar coupling constant was verified through nuclear quadrupole resonance[29] and a previous computational study[31].

DFT calculations of $LaTiO_3$ are complicated by the strong electron correlation at the La^{3+} and Ti^{3+} sites. This requires a special approach (LDA+U)[31] that is inconsistent with the rest of the DFT calculations reported in this work, and hence DFT calculations of $LaTiO_3$ were not performed.

The ellipsoid fitting the LaO_8 polyhedron is triaxial, with e_a = 2.384 ± 0.001 Å, e_b = 2.462 ± 0.001 Å, and e_c = 2.872 ± 0.001 Å. The ellipsoid is quite distorted from spherical symmetry, with ϵ = 0.190 ± 0.001, and a prolate character of 0.59 ± 0.01. The largest semi major axis is parallel with the crystallographic c axis, and is directed towards neighbouring LaO_8 polyhedra (Figure S27).

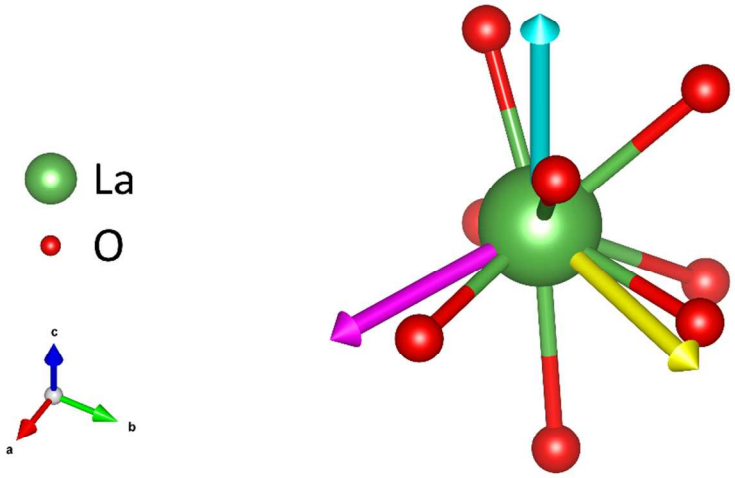

Figure S27. First coordination sphere of LaO_8 in $LaTiO_3$. The e_a, e_b, and e_c semi major axes are in yellow, magenta, and teal respectively.

Lanthanum Niobate

$LaNbO_4$ has been thoroughly investigated using ^{139}La ssNMR by Spencer et al.;[5] we will not duplicate their efforts here. $LaNbO_4$ has a monoclinic crystal structure of space group I2/c with 4 formula units per unit cell.[32] The lanthanum environment in $LaNbO_4$ is eightfold coordinate, with four pairs of La-O bonds with lengths 2.48 Å, 2.49 Å, 2.50 Å, and 2.58 Å. The average La-O bond length is 2.50 Å. The lanthanum coordination polyhedron is a distorted square antiprism.

We performed DFT calculations on the room-temperature monoclinic $LaNbO_4$ crystal structure.[32] Our DFT calculations yield a C_Q of 39.5 MHz and η of 0.50, in good agreement with the experimental values reported by Spencer et al. (C_Q = 36 ± 2 MHz, η = 0.44 ± 0.05)[5]. Our computed EFG parameters have approximately the same deviation from experiment as the computed values reported by Spencer et al. (calculated C_Q = 33.8 MHz, η = 0.38), albeit in the opposite direction.

The ellipsoid used to fit the LaO_8 coordination polyhedron is triaxial, with e_a = 2.419 ± 0.001 Å, e_b = 2.478 ± 0.001 Å, and e_c = 2.606 ± 0.001 Å. The ellipsoid span indicates a moderate level of distortion with ϵ = 0.075 ± 0.001. The ellipsoid is somewhat prolate, with a character of 0.32 ± 0.01. While the longest semi major axis of the ellipsoid is parallel to the crystallographic b axis, the other semi major axes are not aligned with any particular structural feature (Figure S28).

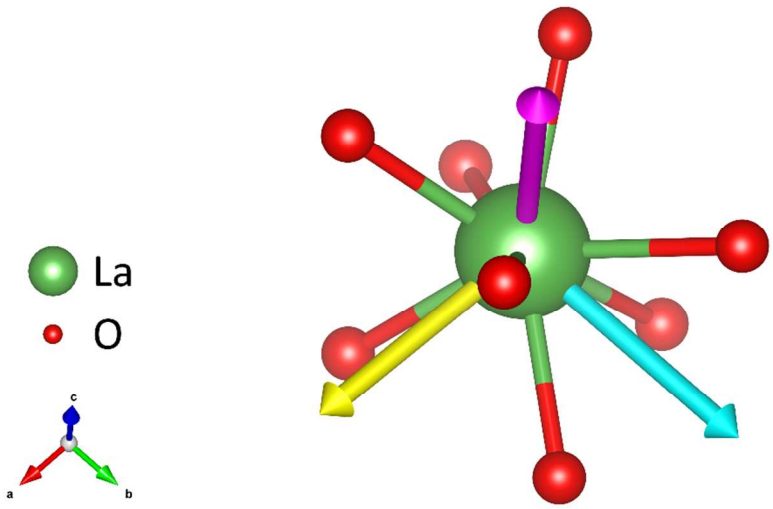

Figure S28. First coordination sphere of LaO_8 in $LaNbO_4$. The e_a, e_b, and e_c semi major axes are in yellow, magenta, and teal respectively.

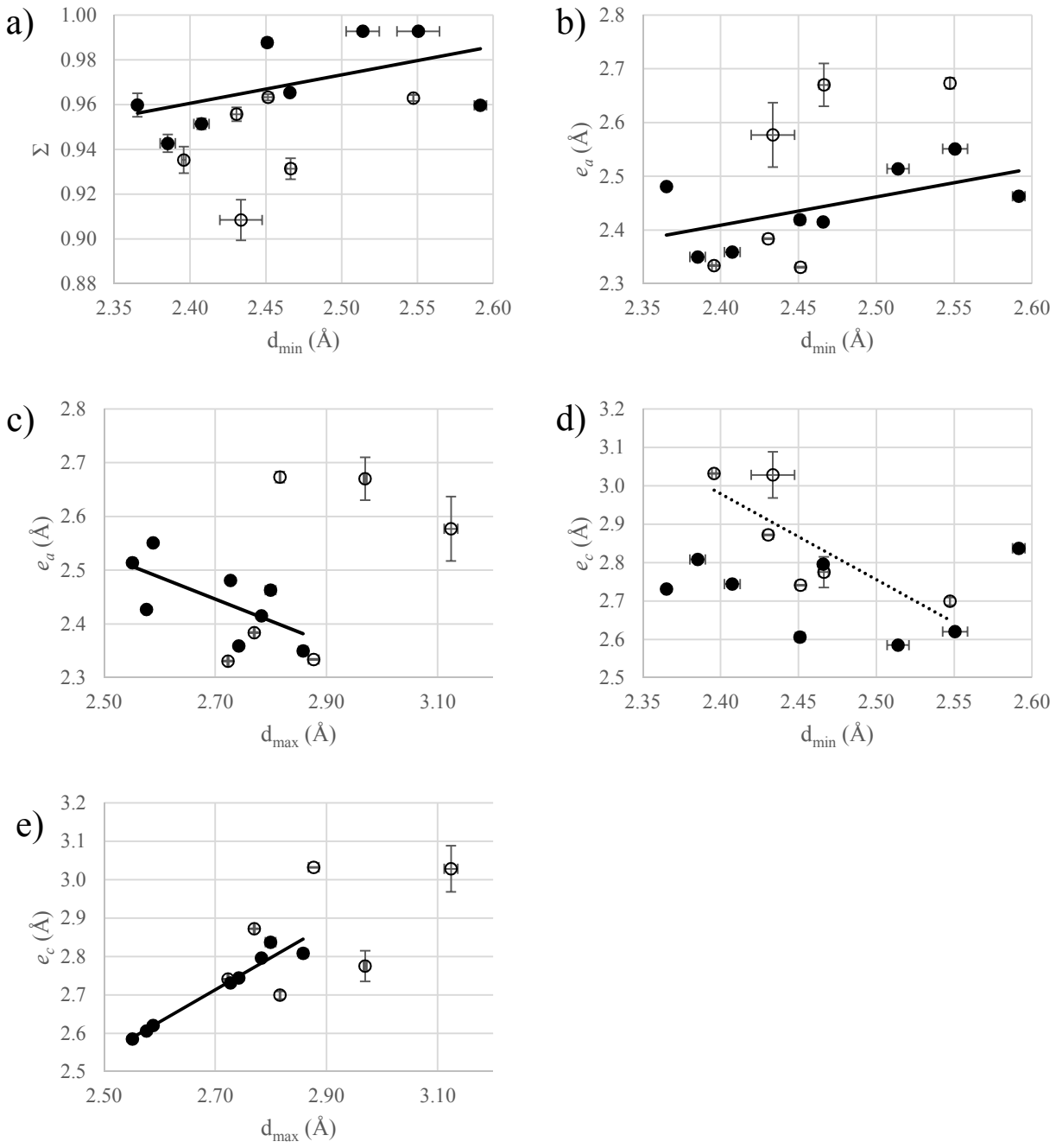

Figure S29. Relationship between sphericity (Σ), ellipsoid expression (ϵ), the shortest ellipsoid semi major axis (e_a), and the longest semi major axis (e_c) and: d_{min} (a, b, d); and d_{max} (c, e). Filled circles (●) indicate compounds of the non-$LaMO_3$ family, while open circles (○) indicate $LaMO_3$ compounds. The solid lines indicate the relationship between the respective distortion parameter and the bond length of the non-$LaMO_3$ family, with: a) $\Sigma = 2.78\frac{1}{\text{Å}} \cdot d + 0.23$ (R^2 =0.38); b) $e_c = 0.67 \cdot d_{min} + 0.81$ Å (R^2 = 0.36); c) $e_a = -1.08 \cdot d_{max} + 5.35$ Å (R^2 = 0.44); e) $e_c = 1.14 \cdot d_{max} - 0.39$Å ($R^2$ = 0.95). The dotted line in d) indicates the relationship between e_c and the minimum La-O bond length of the $LaMO_3$ family, with $e_c = -0.28 \cdot d_{max} + 3.25$Å ($R^2$ = 0.62).

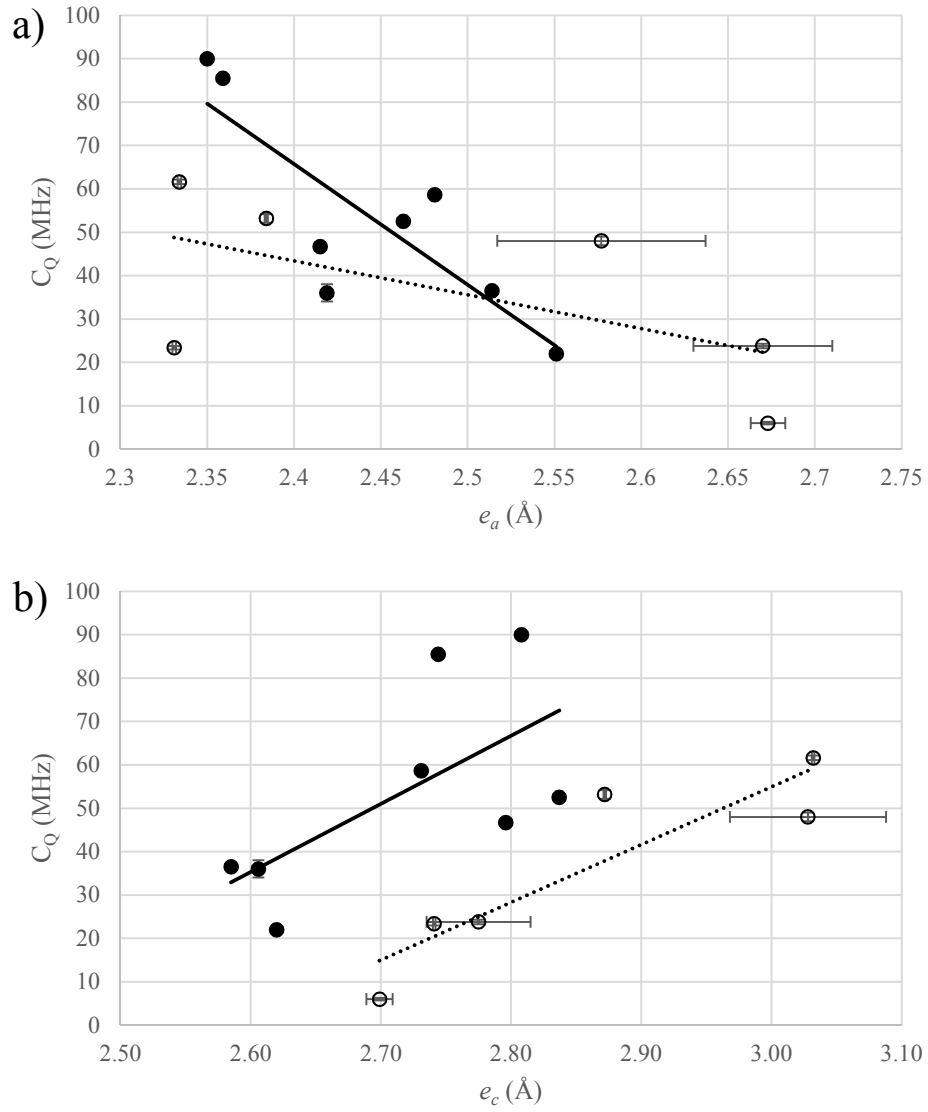

Figure S30. Relationship between ^{139}La C_Q and: a) shortest ellipsoid semi major axis (e_a); b) longest semi major axis (e_c). Filled circles (●) indicate compounds of the non-$LaMO_3$ family, while open circles (○) indicate $LaMO_3$ compounds. The solid lines in indicate the relationship between ^{139}La C_Q and the respective distortion parameter of the non-$LaMO_3$ compounds, with: a) C_Q = -278 $\frac{MHz}{Å} \cdot e_a$ + 734 MHz (R^2 = 0.69); b) C_Q= 157 $\frac{MHz}{Å} \cdot e_c$ - 373 MHz (R^2 = 0.42). The dotted lines indicate the relationship between ^{139}La C_Q and the respective distortion parameter of the $LaMO_3$ compounds, with: a) $C_Q = -78 \frac{MHz}{Å} \cdot e_a + 230$ MHz (R^2 = 0.35); and b) $C_Q = 133 \frac{MHz}{Å} \cdot e_c - 344$ MHz (R^2 = 0.81).

References for Supporting Information

(1) Lucas, S.; Champion, E.; Bregiroux, D.; Bernache-Assollant, D.; Audubert, F. Rare Earth Phosphate Powders $RePO_4 \cdot nH_2O$ (Re=La, Ce or Y) - Part I. Synthesis and Characterization. *J. Solid State Chem.* **2004**, *177*, 1302–1311.

(2) Poston, J. a.; Siriwardane, R. V.; Fisher, E. P.; Miltz, A. L. Thermal Decomposition of the Rare Earth Sulfates of cerium(III), cerium(IV), lanthanum(III) and samarium(III). *Appl. Surf. Sci.* **2003**, *214*, 83–102.

(3) Pyykkö, P. Year-2008 Nuclear Quadrupole Moments. *Molecular Physics*. August 20, 2008, pp 1965–1974.

(4) Bastow, T. J. 139La Nuclear Magnetic Resonance Characterisation of La_2O_3 and $La_{1-x}Sr_xMO_3$ Where M = Cr, Mn or Co. *Solid State Nucl. Magn. Reson.* **1994**, *3*, 17–22.

(5) Spencer, L.; Coomes, E.; Ye, E. Structural Analysis of Lanthanum-Containing Battery Materials Using ^{139}La Solid-State NMR. *Canadian Journal of Chemistry*. 2011, pp 1105–1117.

(6) Schiller, G. Die Kristallstrukturen von Ce_2O_3 (A-Form), $LiCeO_2$ Und CeF_3, Ein Beitrag Zur Kristallchemie Des Dreiwertigen Cers., Universitaet Karlsruhe, 1985.

(7) Dithmer, L.; Lipton, A. S.; Reitzel, K.; Warner, T. E.; Lundberg, D.; Nielsen, U. G. Characterization of Phosphate Sequestration by a Lanthanum Modified Bentonite Clay: A Solid-State NMR, EXAFS, and PXRD Study. *Environ. Sci. Technol.* **2015**, 150323063204005.

(8) Mooney, R. C. L. X-Ray Diffraction Study of Cerous Phosphate and Related Crystals. I. Hexagonal Modification. *Acta Crystallogr.* **1950**, *3*, 337–340.

(9) Mesbah, A.; Clavier, N.; Elkaim, E.; Kacem, I. Ben; Szenknect, S.; Dacheux, N. Monoclinic Form of the Rhabdophane Compounds : **2014**, *28*.

(10) Yunxiang Ni; Hughes, J. M.; Mariano, A. N. Crystal Chemistry of the Monazite and Xenotime Structures. *Am. Mineral.* **1995**, *80*, 21–26.

(11) Kroeker, S.; Stebbins, J. F. Three-Coordinated Boron-11 Chemical Shifts in Borates.

Inorg. Chem. **2001**, *40*, 6239–6246.

(12) Sigaev, V. N.; Dechev, A. V.; Kadyshman, S. L.; Al'takh, O. L.; Stefanovich, S. Y.; Molev, V. I. Glasses in the La_2O_3-B_2O_3-SiO_2 System and Crystallization of the Ferroelectric LaBSiO5 Phase. *Glas. Phys. Chem.* **1996**, *22*, 1.

(13) Nakatsuka, A.; Ohtaka, O.; Arima, H.; Nakayama, N.; Mizota, T. Aragonite-Type Lanthanum Orthoborate, $LaBO_3$. *Acta Crystallogr. Sect. E Struct. Reports Online* **2006**, *62*, i103–i105.

(14) Abdullaev, G. K.; Dzhafarov, G. G.; Mamedov, K. S. Crystal Structure of Lanthanum Orthoborate. *Azerbaidzhanskii Khimicheskii Zhurnal* **1976**, 117–120.

(15) Samygina, V. R.; Genkina, E.; Maksimov, B. A.; Leonyuk, N. I. Crystal Structure of La-Analog of Stilvellite. *Kristallografiya* **1993**, *38*, 61–65.

(16) Ono, Y.; Takayama, K.; Kajitani, T. X-Ray Diffraction Study of $LaBSiO_5$. *J. Phys. Soc. Japan* **1996**, *65*, 3224–3228.

(17) Hamaed, H.; Lo, A. Y. H.; Lee, D. S.; Evans, W. J.; Schurko, R. W. Solid-State ^{139}La and ^{15}N NMR Spectroscopy of Lanthanum-Containing Metallocenes. *J. Am. Chem. Soc.* **2006**, *128*, 12638–12639.

(18) Sherry, E. G. The Structure of $Pr_2(SO_4)_3 \cdot 8H_2O$ and $La_2(SO_4)_3 \cdot 9H_2O$. *J. Solid State Chem.* **1976**, *19*, 271–279.

(19) Shinn, D. B.; Eick, H. A. Crystal Structure of Lanthanum Carbonate Octahydrate. *Inorg. Chem.* **1968**, *7*, 1340–1345.

(20) Michiba, K.; Tahara, T.; Nakai, I.; Miyawaki, R.; Matsubara, S. Crystal Structure of Hexagonal $RE(CO_3)OH$. *Zeitschrift für Krist.* **2011**, *226*, 518–530.

(21) Fleming, P.; Farrell, R. A.; Holmes, J. D.; Morris, M. A. The Rapid Formation of $La(OH)_3$ from La_2O_3 Powders on Exposure to Water Vapor. *J. Am. Ceram. Soc.* **2010**, *93*, 1187–1194.

(22) Beall, G. W.; Milligan, W. O.; Wolcott, H. a. Structural Trends in the Lanthanide Trihydroxides. *J. Inorg. Nucl. Chem.* **1977**, *39*, 65–70.

(23) Khidirov, I.; Om, V. T. Localization of Hydrogen Atoms in Rare Earth Metal Trihydroxides R $(OH)_3$. *Phys. Status Solidi* **1993**, *140*, K59–K62.

(24) Dupree, R.; Lewis, M. H.; Smith, M. E. A High-Resolution NMR Study of the Lanthanum-Silicon-Aluminum-Oxygen-Nitrogen System. *J. Am. Chem. Soc.* **1989**, *111*, 5125–5132.

(25) Lehnert, H.; Boysen, B.; Schneider, S. J.; Frey, F.; Hohlwein, D.; Radaelli, P.; Ehrenberg, H. A Powder Diffraction Study of the Phase Transition in $LaAlO_3$. *Zeitschrift für Krist.* **2000**, *215*, 536.

(26) Thornton, G.; Tofield, B. C.; Hewat, A. W. A Neutron Diffraction Study of $LaCoO_3$ in the Temperature Range $4.2 < T < 1248$ K. *J. Solid State Chem.* **1986**, *61*, 301–307.

(27) Zajtseva, Z. A.; Litvin, A. L.; Ostapenko, S. S. Crystal-Structure Of Lanthanum Chromite. *Dopovidi Akad. Nauk Ukr. Rsr Seriya B-Geologichni Khimichni Ta Biol. Nauk.* **1977**, *12*, 1094–1096.

(28) Tezuka, K.; Hinatsu, Y.; Nakamura, A.; Inami, T.; Shimojo, Y.; Morii, Y. Magnetic and Neutron Diffraction Study on Perovskites $La_{1-x}Sr_xCrO_3$. *J. Solid State Chem.* **1998**, *410*, 404–410.

(29) Furukawa, Y.; Okamura, I.; Kumagai, K.; Goto, T.; Fukase, T.; Taguchi, Y.; Tokura, Y. Electronic Correlations on the Verge of the Mott Transition in $La_{1-x}Sr_xTiO_3$ by $^{47/49}$Ti and ^{139}La Nuclear Magnetic Resonance. *Phys. Rev. B* **1999**, *59*, 10550–10558.

(30) Stramare, S.; Thangadurai, V.; Weppner, W. Lithium Lanthanum Titanates: A Review. *Chem. Mater.* **2003**, *15*, 3974–3990.

(31) Zwanziger, J. First-Principles Study of the Nuclear Quadrupole Resonance Parameters and Orbital Ordering in $LaTiO_3$. *Phys. Rev. B* **2009**, *79*, 1–4.

(32) Huse, M.; Skilbred, A. W. B.; Karlsson, M.; Eriksson, S. G.; Norby, T.; Haugsrud, R.; Knee, C. S. Neutron Diffraction Study of the Monoclinic to Tetragonal Structural Transition in $LaNbO_4$ and Its Relation to Proton Mobility. *J. Solid State Chem.* **2012**, *187*, 27–34.